




Novel and recurrent variants of *ATP2C1* identified in patients with Hailey-Hailey disease

J. Sawicka¹ · A. Kutkowska-Kaźmierczak¹ · K. Woźniak² · A. Tysarowski³ · K. Osipowicz² · J. Poznański⁴ · A. M. Rygiel¹ · N. Braun-Walicka¹ · K. Niepokój¹ · J. Bal¹ · C. Kowalewski² · K. Wertheim-Tysarowska¹ 

Received: 22 October 2019 / Revised: 22 October 2019 / Accepted: 3 January 2020 / Published online: 25 January 2020
© The Author(s) 2020

Abstract

Hailey-Hailey disease (HHD) is a rare, late-onset autosomal dominant genodermatosis characterized by blisters, vesicular lesions, crusted erosions, and erythematous scaly plaques predominantly in intertriginous regions. HHD is caused by *ATP2C1* mutations. About 180 distinct mutations have been identified so far; however, data of only few cases from Central Europe are available. The aim was to analyze the *ATP2C1* gene in a cohort of Polish HHD patients. A group of 18 patients was enrolled in the study based on specific clinical symptoms. Mutations were detected using Sanger or next generation sequencing. In silico analysis was performed by prediction algorithms and dynamic structural modeling. In two cases, mRNA analysis was performed to confirm aberrant splicing. We detected 13 different mutations, including 8 novel, 2 recurrent (p.Gly850Ter and c.325-3 T > G), and 6 sporadic (c.423-1G > T, c.899 + 1G > A, p.Leu539Pro, p.Thr808TyrfsTer16, p.Gln855Arg and a complex allele: c.[1610C > G;1741 + 3A > G]). In silico analysis shows that all novel missense variants are pathogenic or likely pathogenic. We confirmed pathogenic status for two novel variants c.325-3 T > G and c.[1610C > G;1741 + 3A > G] by mRNA analysis. Our results broaden the knowledge about genetic heterogeneity in Central European patients with *ATP2C1* mutations and also give further evidence that careful and multifactorial evaluation of variant pathogenicity status is essential.

Keywords Hailey-Hailey disease · *ATP2C1* · Genodermatosis

Introduction

Hailey-Hailey disease (HHD, OMIM 16960, or Benign Chronic Pemphigus.) is a rare (incidence 1:50000) autosomal dominant genodermatosis. The symptoms, aggravating

The data that support the findings of this study are available from the corresponding author upon reasonable request.

Communicated by: Michal Witt

✉ K. Wertheim-Tysarowska
katarzyna.wertheim@imid.med.pl

- ¹ Medical Genetics Department, Institute of Mother and Child, Kasprzaka 17a, 01-211 Warsaw, PL, Poland
- ² Department of Dermatology and Immunodermatology, Medical University of Warsaw, Koszykowa 82A, 00-001 Warsaw, PL, Poland
- ³ Translational and Molecular Oncology Department, Maria Skłodowska-Curie Memorial Cancer Center and Institute of Oncology, W. K. Roentgena 5, 02-781 Warsaw, PL, Poland
- ⁴ Institute of Biochemistry and Biophysics, Polish Academy of Sciences, Pawińskiego 5A, 02-106 Warsaw, PL, Poland

periodically, onset in third–fourth decade include blisters, vesicular lesions, crusted erosions, and erythematous scaly plaques, which occur mainly on groins, axillae, neck, and other intertriginous areas, and mucosa may also be involved. Lesions may be odorous and painful and lead to mobility affecting fissures (Li et al. 2016; Zamiri and Munro 2016). In histopathological findings, suprabasilar and intraepidermal keratinocyte acantholysis with a “dilapidated brick wall” appearance is due to abnormal epidermal Ca²⁺ distribution by secretory pathway Ca(2+) ATPase 1 (hSPCA1) caused by mutation in its gene: calcium-transporting ATPase type 2C member 1 (*ATP2C1*) (Cheng et al. 2010; Micaroni et al. 2016; Cialfi et al. 2016). Importantly, *ATP2C1* is expressed in all tissues, although HHD clinical symptoms are solely isolated to the skin. Four isoforms differing by alternative processing of the C-terminus are produced, but only few of *ATP2C1* mutations localized beyond the core of 26 exons are present in each transcript (Nellen et al. 2017). The majority of *ATP2C1* mutations lead to a premature termination codon (PTC); thus the dominant inheritance pattern of HHD seems to result from haploinsufficiency. Nevertheless, as around 1/3

of mutations lead to missenses or in-frame rearrangements, other mechanisms may be involved (Dobson-Stone et al. 2002; Kitajima 2002). Thus, to understand the pathophysiological molecular mechanism of HHD, further investigation is required. Worldwide, only about 300 individuals have been described so far with 179 distinct *ATP2C1* variants (Nellen et al. 2017). The majority of them are Asians, and only few cases from Central Europe were published, including a not genotyped case report from Poland (Rącz et al. 2005; Sudbrak et al. 2000; Chlebicka et al. 2012).

Herein, we report the results of the first genetic investigation in 18 Polish HHD patients together with characterization of splicing mutations and in silico structural dynamic modeling of novel missense mutations.

Patients and methods

Eighteen probands of Polish descent (Table 1) with clinical HHD manifestation (according to Matsuda et al. (2014)) have been enrolled in the study, together with their relatives, if available. The average age at diagnosis was 29 years old (range: 15–40). All patients gave informed consent for participation.

All coding exons of *ATP2C1* were analyzed using Sanger sequencing (primers and PCR conditions available on request) or panel next generation sequencing (customized KAPA Library Preparation Kit - Roche) using MiSeq (Illumina). The variants were annotated against NCBI RefSeq: NM_014382.3 and checked for presence in the GnomAD, ClinVar, HGMD Professional and *ATP2C1* LOVD v.3.0 databases.

Novel missense mutations were analyzed using in silico algorithms: DANN, MutationTaster, FATHMM, FATHMM-MKL, GERP, MutationAssessor, SIFT, Provean, and PolyPhen2, classified according to ACMG guidelines (Richards et al. 2015) and visualized using dynamic structural modeling (Yasara Structure Package v.15.7.12). Briefly, isoform 1a of hSPCA1 (NP_055197.2) was modeled by homology, using eight closest templates identified in RCSB Protein Data Bank (PDB) records, IDs: 3N5K, 4BEW, 1WPG, 2YN9, 2YFY, 2ZZE, 4RET, and 4HYT. For each template, up to five alternative sequential alignments have been tested. Finally, the best scored models were built on the basis of 1WPG (37.2% of sequence identity and 56.7% of sequence similarity within 802 residues of 919 being aligned) and 3N5K (36.8%, 56.2%, and 810, respectively) PDB records. However, the final hybrid model, which combines the optimal parts of the top models, was scored substantially higher than the latter and thus was further used.

Novel intronic mutations were evaluated with the use of three splice site prediction algorithms: MaxEnt, NNSPLICE, and HSF. In order to confirm the putative cryptic splicing of mutations c.325-3 T > G and c.1741 + 3A > G, RNA was

isolated from peripheral blood leukocytes, reverse transcribed, and PCR amplified and analyzed using Sanger sequencing (Fig. 1). As negative and positive controls, we included RNA isolated from a healthy person and from a HHD patient with the already known mutation c.1308 + 1G > T.

Results

ATP2C1 variants were detected in 17/18 probands, resulting in a detection frequency of 94%. Overall, we detected 13 different heterozygous *ATP2C1* variants, (6 missense or nonsense, 3 splice site, 1 complex allele (missense and intronic *in cis*), and 3 deletions or duplications). Eight of them (8/13, 61%, Table 1) are novel, i.e., c.2548G > T, c.325-3 T > G, c.423-1G > T, c.899 + 1G > A, c.1616 T > C, c.2408_2420dup, c.2564A > G, and a complex allele: c.[1610C > G;1741 + 3A > G]. Identified mutations localize in the following exons: 26 (2/13), 18 (3/13), and (single variant each) in 7, 8, 12, 21, 23, and 25 and introns 4, 6, and 11.

The molecular dynamic modeling or/and in silico prediction analysis (Table 2) together with mRNA analysis of putative splicing mutations (Fig. 1) enabled us to confirm the likely pathogenic status of these novel variants. Precisely, novel c.325-3 T > G, c.1741 + 3A > G, and recurrent c.1308 + 1G > T mutations cause in-frame skipping of exons 5, 18, and 15, respectively, which seems to severely affect the protein structure.

Discussion

The majority of mutations (61%) identified in this study have never been reported before, including two recurrent novel splice site c.325-3 T > G (intron 4) and nonsense c.2548G > T (exon 26) mutations, identified in 2/17 (12%) and 4/17 (24%) in different Polish families, respectively. This could suggest specific founder mutations in this ethnic population. All *ATP2C1* missense mutations are localized in exons 8, 12, 18, and 26, which is partially in concordance with previous observations clustering in exons 12, 13, 18, 21 and 23 (Micaroni et al. 2016).

Half (4/8) of the novel mutations could easily be classified as pathogenic due to introduction of a premature stop codon (p.Gly850Ter, p.Thr808TyrfsTer16) or change in the conserved consensus sequence of the canonical splice sites (c.423-1G > T, c.899 + 1G > A). The novel missense mutations, p.Gln855Arg, p.Leu539Pro and the p.Thr537Arg detected *in cis* with 1741+3A>G, were analysed using molecular dynamic modeling and standard in silico tools.

Molecular dynamic modeling showed that conversion of Gln855 into Arg would distort the transmembrane helical structure and form a positively charged region located in the

Table 1 Results of genotyping

Fam. No.	Chr3(GRCh37): HGVS ver.15.11 NP_055197.2: NM_014382.3:	HGVS ver.15.11 c.325-3 T>G	Localization	Putative protein domain	No of probands (and family data)	Classification ACMG	Prediction algorithms	Additional data
Novel mutations								
1, 2	g.130656269 T>G p.Ala109 Gln120del†	c.325-3 T>G	Intron 4	M2	2: detected in two distinct families (family 1: the first case in the family, the young-adult son of the patient have some slight clinical symptoms, but did not agree for clinical evaluation and genetic test, family 2 - no data)	Likely Pathogenic (PM4, PM2, PP3, PP4)	MaxEnt: – 100.0% NNSPLICE: – 99.1% HSF: – 3.1%	mRNA analysis performed
3	g.130660434G>T p.?	c.423-1G>T	Intron 6	S2 or A	1 (DNA of affected son of the proband not analyzed)	Pathogenic (PVS1, PM2, PP3)	MaxEnt: – 100.0% NNSPLICE: – 100.0% HSF: – 100.0%	Canonical splice site
4	g.130678186G>A p.?	c.899 + 1G>A	Intron 11	M4	1 (mutation present in proband and in his affected father)	Pathogenic (PVS1, PM2, PP3)	MaxEnt: – 100.0% NNSPLICE: – 100.0% HSF: – 100.0%	Canonical splice site
5	g.130698132C>G p.Thr537Arg	c.1610C>G	Exon 18	N	1 (mutations in cis present in patient and his affected mother)	Likely Pathogenic (PM1, PM2, PP2, PP3)	PolyPhen-2: Probably damaging (score: Hum Div 0.985/1, Hum Var: 0.924/1) SIFT (v6.2.0): Deleterious (score: 0.03, median: 3.58) MutationTaster (v2013): disease causing (p value: 1)	In silico modeling performed
5	g.130698266A>G p.Val524 Ile580del†	c.1741 + 3A>G	Intron 18	N		Likely Pathogenic (PM4, PM2, PP3, PP4)	MaxEnt: – 100.0% NNSPLICE: – 90.9% HSF: – 23.2%	mRNA analysis performed
6	g.130698138 T>C p.Leu539Pro	c.1616 T>C	Exon 18	N	1 (no family data available)	Likely Pathogenic (PM1, PM2, PP2, PP3)	PolyPhen-2: Probably damaging (score: Hum Div 0.992/1, Hum Var: 0.936/1) SIFT (v6.2.0): Tolerated (score: 0.05, median: 3.58) MutationTaster (v2013): disease causing (p value: 1)	In silico modeling performed
7	g.130717154_130717166dup c.2408_2420dup p.Thr808Tyr16Ter16	c.2408_2420dup	Exon 25	L4	1 (no family data available)	Pathogenic (PVS1, PM2, PP3)	PTC	The new reading frame ends in a STOP codon 16 positions downstream from Thr808

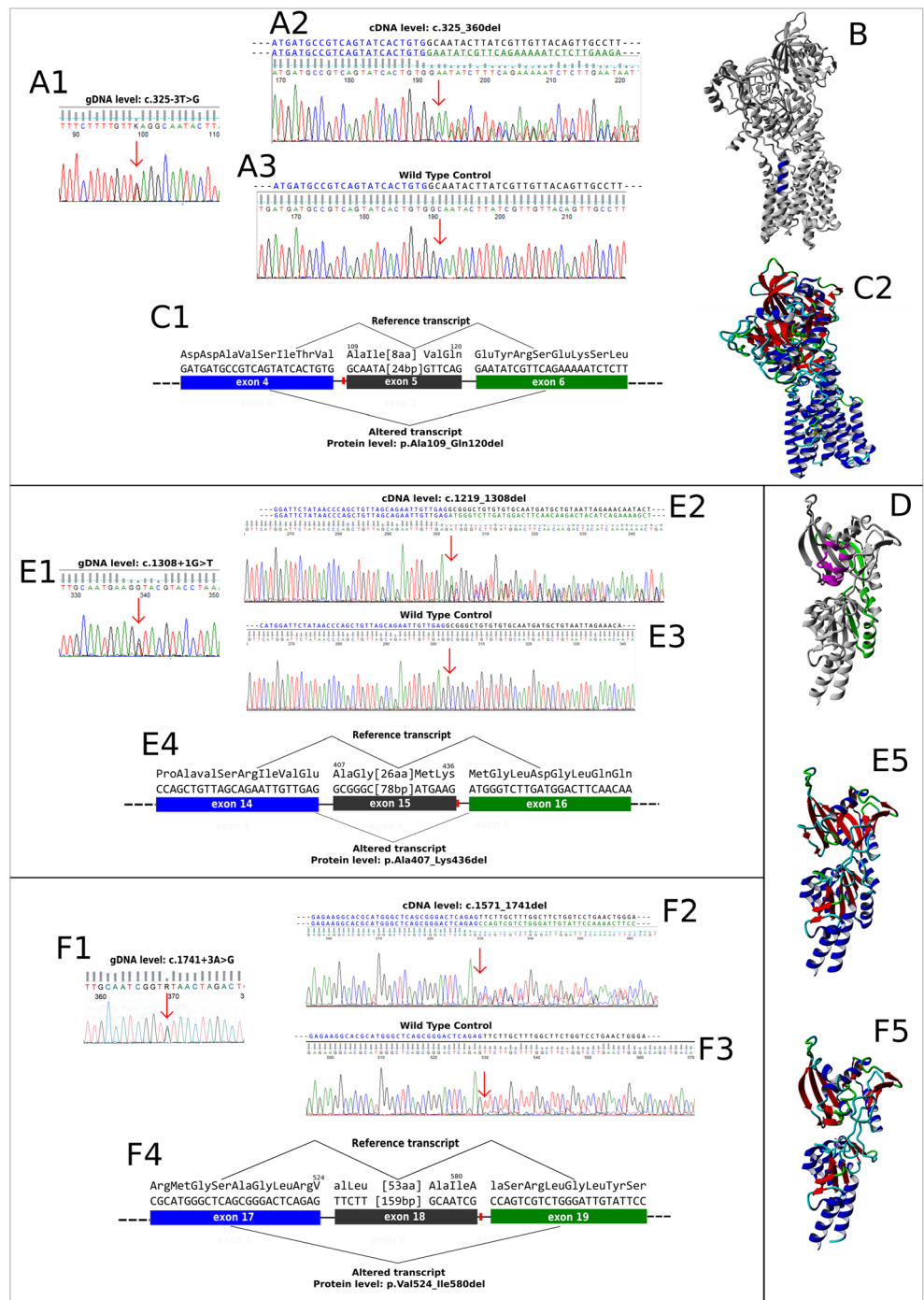
Table 1 (continued)

Fam. No.	Chr3(GRCh37): HGVS ver.15.11 NP_055197.2: NM_014382.3:	HGVS ver.15.11 c.2548G>T c.2564A>G	Putative protein domain	Localization	No of probands (and family data)	Classification ACMG	Prediction algorithms	Additional data
8,9,10,11	g.130718422G>T p.Gly850Ter	c.2548G>T	M9	Exon 26	4 (in 3 cases mutations were present in at least two affected members of the family, in one case the DNA of several affected relatives of the proband were not analyzed 1 (no family data available)	Pathogenic (PVS1, PM2, PP3)	PTC	The mRNA produced might be targeted for nonsense mediated decay (NMD) In silico modeling performed
12	g.130718438A>G p.Gln855Arg	c.2564A>G	M9	Exon 26	1 (no family data available)	Likely Pathogenic (PM2, PP2, PP3)	PolyPhen2:Probably damaging (score: Hum Div 1/1, Hum Var: 1/1) SIFT (v6.2.0): Deleterious (score: 0, median: 3.58) MutationTaster (v2013): disease causing (p value: 1)	
Recurrent mutations								
13	g.130660532dupA	c.519dup	A	Exon 7	1 (mutation present in proband and his child, in whom symptoms appear)	Reference Dobson-Stone et al. 2002		
14	g.130672792G>A	c.659G>A	A	Exon 8	1 (no familial data available)	Nellen et al. 2017		
15	g.130,682,919 T>C	c.1004 T>C	S4	Exon 12	1 (mutation found in proband and 2 affected 1st degree relatives)	Ma et al. 2008		
16	g.130698260A>G	c.1738A>G	N	Exon 18	1 de novo (mutation not detected in parental DNA)	Dobson-Stone et al. 2002		
17	g.130715627dupC	c.2234dup	M6	Exon 23	1 (no familial data available)	Meng et al. 2015		

†according to mRNA analysis

A Actuator domain; N nucleotide-binding domain; S (1–5) stalk helices in the cytoplasm; M (1–10) transmembrane helices

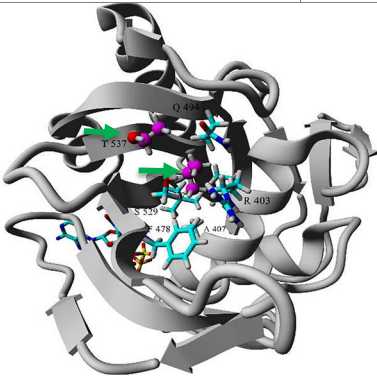
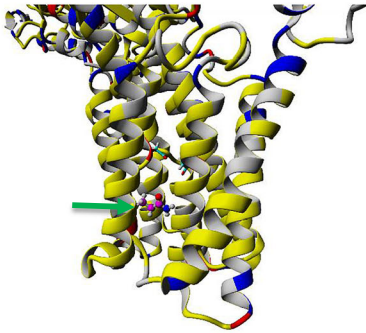
Fig. 1 Results of functional analysis of three splicing mutations in *ATP2C1* gene and modeling of altered protein products (ATPase2C1). Results of DNA genotyping: A1, E1, F1, nucleotide substitutions indicated by red arrows; results of cDNA analysis: A2, E2, F2 (patients samples) and control samples (A3, E3, F3); schematic view of altered and normal transcripts (C1, E4, F4); predicted structure models of ATPase2C1 protein: B – wild type protein showing organization of transmembrane helices with amino acids 109–120 marked in blue; C2 – protein lacking amino acids 109–120; D – wild type protein showing organization of ATP binding domain (amino acids 407–436 marked in magenta, amino acids 524–580 marked in green); E5 – protein lacking amino acids 407–436, F5 – protein lacking amino acids 524–580



proximity of the ion channel, which seemingly would affect protein location and Ca^{2+} transport. The effect of p.Leu539Pro is less clear; however it is possible that this substitution would destabilize hydrophobic core formed between β -sheet structures and hence influence ATPase alpha subunit interactions, which in turn could affect ATP binding, its hydrolysis, and finally ion transportation. Unfortunately, no family data were available for probands with p.Leu539Pro and p.Gln855Arg; thus the genotype-phenotype segregation could not be performed.

The clinical significance of another missense, the p.Thr537Arg in exon 18 is more difficult to evaluate. In GnomAD, no records for p.Thr537Arg can be found. The prediction algorithms (PolyPhen, SIFT, MutationTaster) indicated possible pathogenic effect of p.Thr537Arg. Contradictory to them, dynamic structural modeling showed that this solvent exposed substitution most probably does not result in significant conformational change. Furthermore, the p.Thr537Arg was found *in cis* with a novel, mutation c.1741 + 3A > G in intron 18, which leads to exon 18 in-

Table 2 Results of structural dynamic modeling.

Part B – results of structural modeling				
NAME	p.Thr537Arg	p.Leu539Pro	p.Gln855Arg	
CONSERVATION	moderate	high	high	
structural modeling in Yasara Structure Package (v.15.7.12)	INTERACTIONS	Solvent exposed. Thr537 replacement by Arg may be accommodated without significant change of the protein structure (RMSD for CA atoms of the domain estimated to 0.47Å)	Located in β-sheet proximal to the putative hydrolase site of ATPase alpha subunit Contributes to the strongly packed hydrophobic core build by side chains of Arg 403, Ile 404, Ala 407, Phe 478, Gln 494, Leu 527, Ser 529, Thr 537, Leu 539. Hence, Leu539Pro replacement seem to induce compensation, probably by reorientation of numerous residues (RMSD for CA atoms of the domain estimated to 0.96Å).	Located in the transmembrane helical region. The side chain makes numerous hydrophobic contacts with Ile 852, Ile 859 and with other residues located in the neighboring helices: Met 741, Phe 812, Thr 813, Val 816 and Phe 817. Most of these interactions are lost upon Gln855Arg replacement. Moreover, Gln 855 is proximal to the putative ion transporting channel (Asp, Asp, Asn, Asn), so Gln855Arg replacement most probably will also directly affect Ca transport.
	PREDICTED EFFECT OF SUBSTITUTION	Unfavorable electrostatic interaction with a proximal Arg403 may slightly affect domain protein stability	Disorganization of the hydrophobic core most probably results in a substantial decrease of the protein stability	Distortion of transmembrane helices organization together with positively charged region located in the proximity of ion channel will most probably severely disrupt Ca transport.
POLY-PHEN 2	Probably damaging (score: Hum Div 0.985/1, Hum Var: 0.924/1)	Probably damaging (score: Hum Div 0.992/1, Hum Var: 0.936/1)	Probably damaging (score: Hum Div 1/1, Hum Var: 1/1)	
SIFT	Deleterious (score: 0.02, median: 3.59)	Tolerated (score: 0.06, median: 3.57)	Deleterious (score: 0, median: 3.57)	
MUTATION TASTER	disease causing (p-value: 1)	disease causing (p-value: 1)	disease causing (p-value: 1)	
REGISTERED IN THE OTHER DATABASES	no	no	no	
Schematic representation of the domain. Thr537, Leu539 and Gln855 are viewed as ball and stick models and indicated by green arrows.				

Abbreviations: F - familial, S - sporadic, ND - no data

frame skipping as we have shown by mRNA analysis. Thus, the protein, if at all synthesized, lacks 57 codons including codon 537. This example of a complex allele containing two variants is not reported before, and c.[1610C > G;1741 + 3A > G], which both were assigned as potentially pathogenic by common prediction algorithms, draws attention on an important issue of careful pathogenicity status evaluation, especially when only selected exons are investigated. Importantly, when p.Thr537Arg status was evaluated alone, it was assigned as “likely pathogenic” using ACMG classification (Richards et al. 2015), which later changed into “uncertain significance” when we detected c.1741 + 3A > G and proved its impact on splicing.

Novel c.325-3 T > G and recurrent c.1308 + 1G > T mutations also lead to in-frame exons skipping (of exons 5 and 15, respectively). Moreover, given that skipping of exons 5 and 15 due to other mutations have been described before (Kitajima 2002; Matsuda et al. 2014; Xiao et al. 2019), our

observation indicates that despite distinct molecular lesions, the functional effect of mutations may be similar, which could be significant with regard to the purposes of personalized treatment.

In summary, this is the first report of genetic analysis in Polish HHD patients. Thirteen variants were identified and characterized, including eight unreported before and two recurrent. The results further show heterogeneity in the *ATP2C1* mutational spectrum, with possible ethnic-specificity. Last but not the least, by showing a case of complex allele c.[1610C > G;1741 + 3A > G], we also point that careful in silico and extended molecular analysis is essential with respect to proper interpretation of mutation pathogenicity.

Acknowledgments The authors would like to thank Michel van Geel, Ph.D., for his kind help and comments.

Funding information This study was funded by National Science Center (NCN) grant no: 2014/13/D/NZ5/03304.

Compliance with ethical standards

Conflict of interest The authors declare that they have no conflict of interest.

Ethical approval All procedures performed in studies involving human participants were in accordance with the ethical standards of the institutional and national research committee and with the 1964 Helsinki declaration and its later amendments or comparable ethical standards.

Statement of informed consent Informed consent was obtained from all individual participants included in the study.

Open Access This article is licensed under a Creative Commons Attribution 4.0 International License, which permits use, sharing, adaptation, distribution and reproduction in any medium or format, as long as you give appropriate credit to the original author(s) and the source, provide a link to the Creative Commons licence, and indicate if changes were made. The images or other third party material in this article are included in the article's Creative Commons licence, unless indicated otherwise in a credit line to the material. If material is not included in the article's Creative Commons licence and your intended use is not permitted by statutory regulation or exceeds the permitted use, you will need to obtain permission directly from the copyright holder. To view a copy of this licence, visit <http://creativecommons.org/licenses/by/4.0/>.

References

- Cheng TS, Ho KM, Lam CW (2010) Heterogeneous mutations of the ATP2C1 gene causing Hailey-Hailey disease in Hong Kong Chinese. *J Eur Acad Dermatol Venereol* 24:1202–1206
- Chlebicka I, Jankowska-Konsur A, Maj J et al (2012) Generalized Hailey-Hailey disease triggered by nonsteroidal anti-inflammatory drug-induced rash: case report. *Acta Dermatovenerol Croat* 20:201–203
- Cialfi S, Le Pera L, De Blasio C et al (2016) The loss of ATP2C1 impairs the DNA damage response and induces altered skin homeostasis: consequences for epidermal biology in Hailey-Hailey disease. *Sci Rep* 6:31567
- Dobson-Stone C, Fairclough R, Dunne E, Brown J et al (2002) Hailey-Hailey disease: molecular and clinical characterization of novel mutations in the ATP2C1 gene. *J Invest Dermatol* 118:338–343
- Kitajima Y (2002) Mechanisms of desmosome assembly and disassembly. *Clin Exp Dermatol* 27:684–690
- Li H, Chen L, Mei A, Chen L et al (2016) Four novel ATP2C1 mutations in Chinese patients with Hailey-Hailey disease. *J Dermatol* 43:1197–1200
- Ma YM, Zhang XJ, Liang YH, Ma L, Sun LD, Zhou FS et al (2008) Genetic diagnosis in a Chinese Hailey-Hailey disease pedigree with novel ATP2C1 mutation. *Arch Dermatol Res* 300:203–207
- Matsuda M, Hamada T, Numata S et al (2014) Mutation-dependent effects on mRNA and protein expressions in cultured keratinocytes of Hailey-Hailey disease. *Exp Dermatol* 23:514–516
- Meng L, Gu Y, Du XF et al (2015) Two novel ATP2C1 mutations in patients with Hailey-Hailey disease and a literature review of sequence variants reported in the Chinese population. *Genet Mol Res* 14:19349–19359
- Micaroni M, Giacchetti G, Plebani R et al (2016) ATP2C1 gene mutations in Hailey-Hailey disease and possible roles of SPCA1 isoforms in membrane trafficking. *Cell Death Dis* 7:e2259
- Nellen RG, Steijlen PM, van Steensel MA, Vreeburg M et al (2017) Mendelian disorders of cornification caused by defects in intracellular calcium pumps: mutation update and database for variants in ATP2A2 and ATP2C1 associated with Darier disease and Hailey-Hailey disease. *Hum Mutat* 38:343–356
- Rácz E, Csikós M, Kárpáti S (2005) Novel mutations in the ATP2C1 gene in two patients with Hailey-Hailey disease. *Clin Exp Dermatol* 30:575–577 Retrieved from https://books.google.pl/books?id=EyyCwAAQBAJ&pg=SA66-PA10&dq=HHD+hailey-hailey+disease+clinical+recognition&hl=pl&sa=X&ved=0ahUKewja_aLG2p3hAhWKw6YKHUMqALYQ6AEILDAA#v=onepage&q=HHD%20hailey-hailey%20disease%20clinical%20recognition&f=false Accessed May 14, 2019
- Richards S, Aziz N, Bale S, Bick D et al (2015) Standards and guidelines for the interpretation of sequence variants: a joint consensus recommendation of the American College of Medical Genetics and Genomics and the Association for Molecular Pathology. *Genet Med* 17:405–424
- Sudbrak R, Brown J, Dobson-Stone C et al (2000) Hailey-Hailey disease is caused by mutations in ATP2C1 encoding a novel Ca²⁺ pump. *Hum Mol Genet* 9:1131–1140
- Xiao H, Huang X, Xu H et al (2019) A novel splice-site mutation in the ATP2C1 gene of a Chinese family with Hailey-Hailey disease. *J Cell Biochem* 120:3630–3636
- Zamiri M, Munro CS (2016) Inherited acantholytic disorders. In: Griffiths C, Barker J, Bleiker T, Chalmers R, Creamer D (eds) *Rook's Textbook of Dermatology*. Wiley Blackwell, Hoboken

Publisher's note Springer Nature remains neutral with regard to jurisdictional claims in published maps and institutional affiliations.